SLAC–PUB–7896
ICHEP–PA07 #183
July 1998

# Inclusive Search for $b \to sg$[†]

The SLD Collaboration[**]
Stanford Linear Accelerator Center,
Stanford University, Stanford, CA 94309

## Abstract

We describe an inclusive search for flavor changing neutral current decays of the type $b \to s\ gluon$ in the SLD experiment. Models of $b \to sg$ indicate that the production of high momentum kaons is enhanced over background from standard $B$ decays. If the branching ratio for $b \to sg$ is $\approx 10\%$, then such an enhancement should have a good signal to background ratio. The analysis makes use of the particle identification and high precision vertexing capabilities of SLD to search for such an enhancement. The data sample consists of 300K hadronic $Z^0$ decays collected between 1993 and 1997.

*Paper Contributed to the XXIXth International Conference on High Energy Physics, July 23-29, 1998, Vancouver, Canada.*

[†]Work supported in part by the Department of Energy contract DE–AC03–76SF00515.

# 1 Introduction

The low measured $B$ semileptonic decay branching ratio (BR) and charm production deficit in $B$ decays compared to theoretical expectations has been a persistent puzzle in $B$ physics. This has left room for $B$ decays from possible mechanisms beyond the Standard Model with BR as large as 10%. In the Standard Model, flavor changing neutral current decays of the type $b \to s\, g^{(*)}$ (including $b \to sg$ and $b \to sq\overline{q}$) have a total branching ratio of $\approx 1\%$ [1]. One hypothesized scenario is that the $b \to sg$ decay is enhanced to a BR of 10% by new physics [2]. Such a scenario is consistent with all existing experimental constraints, including the measured BR($b \to s\gamma$), and would nicely explain the above puzzles.

The fact that a very large $b \to sg$ branching ratio, even as much as 10% is still allowed, is due to the lack of a distinctive experimental signature for the $b \to sg$ decays compared to the normal $b \to c$ hadronic decays. One possible signal is inclusive high momentum $\eta'$ production. CLEO has measured $\eta'$ production in $B$ decays in the range $2.0 < p_{\eta'} < 2.7$ GeV/c at $\sim 6 \times 10^{-4}$ level [3]. $b \to s\, g^{(*)}$ decays are thought to be the most plausible explanation, although it is difficult to relate the observed rate to an inclusive $b \to s\, g^{(*)}$ branching ratio [4]. The surprisingly large BR($B \to \eta' K$) of $\sim 6 \times 10^{-5}$ [5] is also consistent with that expected from enhanced $b \to sg$. However, it has been argued [6] that a rate at this level can be explained by variation of theoretical parameters within the Standard Model.

It is therefore important to search for other direct signals from enhanced $b \to sg$, preferably at a larger inclusive rate to avoid the confusion due to the various more subtle Standard Model backgrounds, e.g. $b \to sq\overline{q}$. A larger inclusive signal may also be easier to relate to the absolute rate of $b \to sg$ production. One alternative signal from $b \to sg$ could be the leading kaon production at high momentum from the $b \to s$ transition. The analogous effect at high energies where high momentum leading kaons in an $s$ jet tend to contain the primary $s$ quark has already been clearly demonstrated [7]. In a JETSET-inspired [8] model of $b \to sg$, [9] it has been verified that the momentum spectrum of kaons produced in $b \to sg$ decays is indeed expected to be significantly stiffer than that of the background from standard $b \to c$ decays.

CLEO has searched for high momentum $K_s^0$ production in $B$ decays [3]. However, the precision was limited by the large continuum background sub-

traction, as well as the reduced production branching ratio and reconstruction efficiency of $K^0_s \to \pi^+\pi^-$.

In this paper, we describe a search for enhanced $b \to sg$ using data from the SLD detector. The search involves studying the high momentum part of the $K^\pm$ spectrum and looking for the expected enhancement from $b \to sg$ decays. Rather than using the $K^\pm$ momentum in the $B$ rest frame, which is rather difficult to measure due to the unknown boost of $B$'s produced in $Z^0$ decay, we use the momentum transverse to the $B$ flight direction ($p_t$). $p_t$ is a Lorentz invariant quantity and is a simple projection of the $K^\pm$ momentum in the B rest frame.

The boost of the $B$ combined with the high quality vertexing capability of SLD allows a very efficient and high purity $b$ tag, as well as clean separation of $B$ decay tracks from primary fragmentation products. Non-$B$ decay backgrounds are therefore negligible. This is a vital advantage compared to the $\Upsilon(4s)$ because it avoids the heavy penalty, both statistically and systematically, which otherwise arises from the non-$B$ background subtraction. Another key factor making this analysis viable at SLD is the excellent particle identification capability of the SLD Cerenkov Ring Imaging Detector, which allows efficient use of the more abundant $K^\pm$ production. The high resolution vertexing capability at SLD and the small and stable SLC interaction point bring further benefits to this analysis by providing precision $B$ flight direction determination and $B$ decay cascade vertex structure distinction to separate $b \to sg$ decays from normal $b \to c$ decays.

# 2 Detector and Data Sample

The SLD experiment collects $Z^0$ decay data from the $e^+e^-$ collisions at the SLAC Linear Collider with a center of mass energy of 91.28 GeV. Charged particle tracking is provided by the Central Drift Chamber (CDC) [10] and a CCD based pixel vertex detector (VXD) [11][12], residing within a uniform axial magnetic field of 0.6T. The vertex detector used in the 1992-1995 run (VXD2) was replaced by an upgrade vertex detector (VXD3) in 1996, which has significantly improved performance. The Liquid Argon Calorimeter (LAC) [13] is used for the triggering and selection of the events, as well as for determination of the event thrust axis.

The reconstructed track momentum resolution is $\frac{\delta p_\perp}{p_\perp} = 0.01 \oplus 0.0026 p_\perp$.

The track impact parameter resolution at high momentum is $11\mu m$ in the $r\phi$ plane and $23\mu m$ ($37\ \mu m$) in the $rz$ plane for VXD3 (VXD2). The impact parameter resolution in both $r\phi$ and $rz$ views are $40\mu m$ ($78\mu m$) at $\frac{P}{sin^{3/2}\theta}$=1 GeV/c for VXD3 (VXD2). The small and stable SLC interaction point in $r\phi$ is tracked continuously averaging over $\sim$30 hadronic $Z^0$ events, with a resulting effective event primary vertex resolution of $5\mu m$ ($7\mu m$ for VXD2). The event primary vertex $z$ location is determined event by event with an average precision for VXD3 (VXD2) of $15\mu m$ ($34\mu m$) for $udsc$ events and $30\mu m$ ($52\mu m$) for $b$ events. A more detailed description of the primary vertex determination procedure can be found in [14].

Central to this analysis is the SLD Cerenkov Ring Imaging Detector (CRID) [15] for particle identification. The barrel CRID uses liquid $C_6F_{14}$ and gaseous $C_5F_{12} + N_2$ as radiators. The Cerenkov photons from both radiators are imaged into time projection chambers (TPC) containing photosensitive gas. This analysis uses data from both barrel CRID gas and liquid radiators for $\pi/K/p$ separation in the 0.8-30 GeV/c momentum region, over the polar angle range of $cos\theta \leq 0.68$. The average detected Cerenkov photon yield for highly relativistic charged particles is 9.2 (12.8) per full ring for gas (liquid) rings. The measured refractive index for the gas (liquid) radiator is 1.00172 (1.282), corresponding to $\pi/K/p$ thresholds of 2.4/8.4/16.0 (0.17/0.62/1.17) GeV/c. The measured gas (liquid) ring angular resolution is 3.8 (13) mrad, consistent with the design value. A detailed description of the particle identification performance can be found in section 4.3.

In this analysis, we use 150,000 hadronic $Z^0$ events from the 1993-1995 run with VXD2 and 150,000 hadronic $Z^0$ events from the 1996-1997 run with VXD3. A set of further hadronic event selection criteria are applied to select the fiducial events:

- Total Visible energy in events from charged tracks $>$ 18 GeV.
- Event thrust axis reconstructed from calorimeter clusters satisfy $|cos\theta_{thrust}| < 0.71$.
- Number of CDC tracks $\geq$ 7.
- CDC,VXD and CRID all in normal operation.

The total number of such hadronic $Z^0$ decays selected in '93-'95 was 82,139 and in '96-'97 it was 76,226.

# 3 Monte Carlo Simulation and $b \to sg$ Model

The $Z^0$ to Hadrons Monte Carlo (MC) events are simulated using the JETSET 7.4 [8] generator framework. The decays of $D^0, D^+, D_s$ mesons and $\Lambda_c$ baryons are simulated according to measured exclusive branching ratios as listed in the particle data group review [16]. The $B$ meson decay simulation is based on the QQ Monte Carlo program from CLEO [17]. Within this model, the semileptonic $B$ decays are simulated using the ISGW [18] form factor model, which provides a good description of the CLEO data [19]. The hadronic $B$ decay model is tuned to reproduce the CLEO inclusive measurements of charm meson production [20], charm baryon production [21] and charmonium production [22]. The momentum spectra of $\pi^{\pm}, K^{\pm}, K^0$ and protons in the $B$ decay rest frame and their overall production rates for average $B_u, B_d$ decays in the MC are in good agreement with the ARGUS measurements [23].

For the evaluation of analysis sensitivity to the $b \to sg$ process, we used the JETSET inspired model [9] with a specific set of parameter choices as a bench mark test. Figure 1 shows the predicted $p_t$ spectrum for $K^{\pm}$'s produced in standard $b \to c$ decays and in $b \to sg$ decays for BR($b \to sg$) = 10% and 15% from this model. The low momentum part of $p_t$ spectrum is clearly unreliable for $b \to sg$ signal extraction due to the uncertainty in various background kaon production sources, such as the $s\overline{s}$ popping rate in the $W$ fragmentation. The low momentum spectrum shape for $b \to sg$ is also not very different from the normal $b \to c$ background. The estimate for the high momentum tail of the normal $b \to c$ background is much more reliable, with very little dependence on model tuning.

For $p_t > 1.8$ GeV/c, the ratio of $b \to sg$ to $b \to c$ approaches unity for BR($b \to sg$) $\approx$ 10% so that a $b \to sg$ signal should appear as a clear excess in this region. Note, however, that the Standard Model level BR($b \to s\, g^{(*)}$) would produce only modest excesses of less than 10% over the $b \to c$ background and so would probably not be visible. For one choice of JETSET tuning and a BR($b \to sg$)=10%, the analysis procedure described in the following sections would produce an excess $9.3 \times 10^{-4}$ per measured $B$. However, the $b \to sg$ model is quite sensitive to the tuning of JETSET and so it is difficult to get a solid prediction for the expected excess that one should observe for a given BR($b \to sg$).

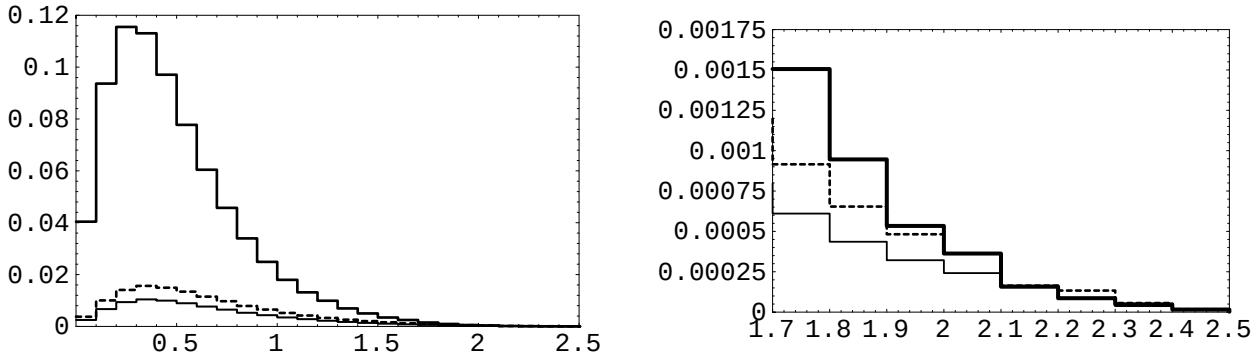


Figure 1: $K^{\pm}$ $p_t$ spectra for standard $b \to c$ (heavy line) and for $b \to sg$ with BR=10% (light line) and BR=15% (dashed line). The first plot shows the whole spectrum and the second shows the high-$p_t$ region.

# 4 Analysis Method

In addition to the main signature of enhancement of high $p_t$ kaons, $b \to sg$ events may also be distinguished from standard $b \to c$ decays by the lack of a charm decay cascade vertex. The traditional vertex detector $b$ tag variables are mainly sensitive to the $B$ lifetime, with the shorter charm lifetime from the $b \to c$ cascade effect present at a secondary level among various other effects. A more direct test of the presence of $b \to c$ cascade internal decay structure is to determine whether all secondary tracks are consistent with coming from the same vertex, eliminating the dependence on the first order $B$ lifetime information. This of course demands high precision vertexing capability to reliably assign each track as primary or $B$ decay and to resolve the rather short charm lifetime.

The data is therefore split into two samples: "1-Vertex" where all tracks identified as coming from the $B$ decay are consistent with coming from a single vertex, and a "2-Vertex" sample for the remaining events with poor single vertex fit probabilty. The 1-vertex sample is expected to be enriched in $b \to sg$ events which would carry most of the high $p_t$ kaon production enhancement. The 2-vertex sample is expected to be depleted of $b \to sg$ events, so that kaon production in the same high $p_t$ range can be used to check the background simulation. Our results will be reported as an excess

or deficit of high $p_t$ $K^{\pm}$'s compared to the expectation from standard $b \to c$ decays.

The analysis proceeds in four steps:

- In each hemisphere, tracks coming from the $B$ decay chain are selected by an inclusive vertex reconstruction method.
- These tracks are fit to single vertex and the hemispheres classified as 1- or 2-vertex.
- Tracks identified as $K^{\pm}$'s are selected
- The $K^{\pm}$ $p_t$ spectra of the 1 and 2 vertex samples are compared to Monte Carlo predictions.

The following sections describe each of these steps in more detail.

## 4.1 Vertex Reconstruction

Track selection and vertex reconstruction is performed as in the SLD $R_b$ measurement and is described in detail in [24]. Briefly, the procedure is as follows. Well measured tracks with vertex detector hits are selected. In each hemisphere, secondary vertices are formed from these "quality" tracks using a topological vertexing technique [25]. The most significant of these vertices that is significantly displaced from the IP is chosen as the "seed". The $B$ flight direction is then defined by the line joining the primary vertex and this secondary vertex. Additional tracks are attached to the vertex if they satisfy the following criteria.

- the 3D closest approach to the flight direction is $<$ 1mm
- the distance along the vertex to this point, L, is $>$0.5 mm
- the $L/D > 0.25$, where D is the secondary vertex decay distance.

The mass of all of these tracks, seed plus attached, is then calculated assuming that each has the mass of the charged $\pi$. A correction is applied to account for neutrals and missing tracks which is based on the total transverse momentum of the vertex tracks to the $B$ flight direction. Finally a cut on

this "$p_t$ corrected mass" is applied at 2 Gev. In Monte Carlo studies, this $b$ selection method had an efficiency of 35% and a purity of 98% in '93-'95 and an efficiency of 48% and a purity of 98% in '96-'97. In '93-'95 data, the number of $b$-tagged hemispheres was 12701 and in '96-'97 it was 13972.

## 4.2 One Vertex Cut

The set of tracks selected as coming from the $B$ decay chain by the above method are then fit to a single vertex. Hemispheres with fit probabilities greater than 0.05 are classified as 1-vertex and the others as 2-vertex. As a check that this method did indeed provide separation between "charmless" and $b \to c$ decays, Monte Carlo events of different types are selected and the cut applied to each set independently. Table 1 shows the results of this study for '93-'95 and for '96-'97.

| $B$ Decay Mode | '93-'95 1-Vertex Fraction | '96-'97 1-Vertex Fraction |
|---|---|---|
| Semi-leptonic | 0.51 | 0.37 |
| Hadronic D + X | 0.49 | 0.33 |
| Double Charm | 0.32 | 0.16 |
| Charmonium + X | 0.79 | 0.76 |
| $b \to sg$ | | 0.72 |

Table 1: Fraction of Monte Carlo events of different types which satisfied the 1-Vertex cut for '93-95 and for '96-'97.

As expected, a large fraction of $b \to c$ decays do not fit to a single vertex due to the finite charm lifetime. For "double charm" ($b \to c\bar{c}s$), where the two charm quarks form separate charm hadrons, a yet smaller fraction pass the cut because two extra separated vertices are available. For charmonium events, the 1 vertex fraction is high due to the lack of separated vertices. Similarly, for $b \to sg$ events generated by the model described in section 3, the efficiency is also quite high. Clearly, the upgraded vertex detector (VXD3) improved the separation of this cut.

The efficiency of the 1-Vertex cut is also checked in the data for $b \to J/\psi + X$ events where the $J/\psi$ decayed to two muons, and the results found to be consistent with the Monte Carlo predictions.

## 4.3 Kaon Identification

To ensure the availability of CRID data for particle identification, the track selection for kaon identification includes further requirements in addition to the standard quality track selection for vertexing. Only tracks with momentum ($p$) greater than 0.8 GeV/c and $|cos\theta| < 0.68$ are used. For tracks that pass through a CRID TPC, an associated minimum ionizing particle signal is requred. Otherwise, for tracks with $p > 2.5$GeV/c, a liquid ring with at least four hits is required.

Charged kaon identification with the CRID is performed using a likelihood technique [26]. For each of the charged particle hypotheses a likelihood is calculated based upon the number of detected photo-electrons and their measured Cerenkov angles compared to the expectations for this hypothesis. This likelihood calculation takes into account the effects of locally measured background including that due to overlapping rings. Particle separation is based upon differences between logarithms of the likelihoods, for pion, kaon and proton hypotheses, combining the gas and liquid information

The kaon identification efficiency of the above procedure is between 50% and 60% for $0.8 < p < 20$ GeV/c and falls off for $p$ above 20 GeV/c. The $\pi \to K$ misidentification rates range from ~1.5% at low momentum to 8-12% at high momentum. The $\pi \to K$ misidentification rates are checked in the data using $K^0_s \to \pi^+\pi^-$ and $\tau$ decay tracks. The Monte Carlo $\pi \to K$ misidentification rates are corrected to match the data. Further details on $K^\pm$ identification in SLD may be found in [27].

## 4.4 $p_t$ Measurement

The measurement of the transverse momentum of each track is done using the $B$ flight direction as defined in section 4.1. Using the vertex direction as a measure of the $B$ flight direction is superior to using, for example, the jet axis because it gives better resolution and it is not biased by high momentum tracks. Figure 2 shows the improved resolution and lack of bias given by the use of vertex direction rather than jet axis from tracks.

As a check that $p_t$ measurement is simulated correctly, the measured spectrum of identified muons was checked against Monte Carlo. Since the lepton production spectrum in B-decays has been well measured [19] and the SLD Monte Carlo has been tuned to match it, the measured $\mu^\pm$ spectrum provides

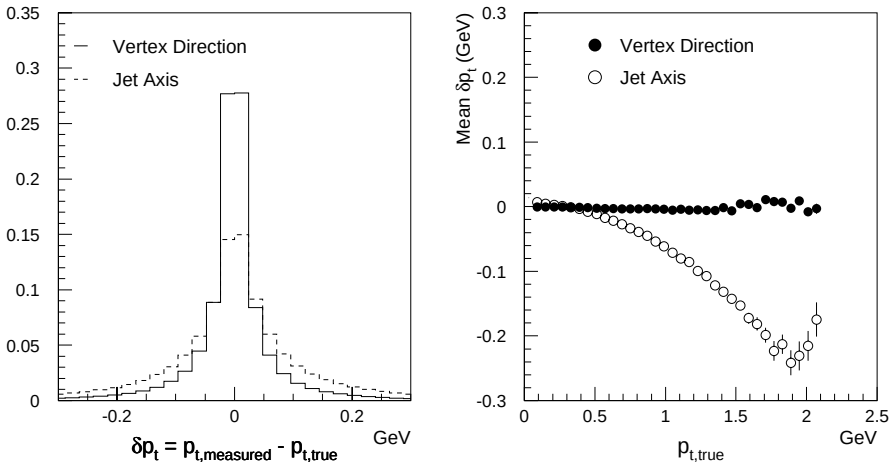


Figure 2: The first plot is a histogram of the difference between measured and true $p_t$ when using the vertex direction and jet axis. The second plot shows the mean of this difference as a function of true $p_t$.

a good way to check the $p_t$ measurement. Figure 3 shows this comparison, with the Monte Carlo normalized to the data by the number of $b$-tagged hemispheres. The good agreement between data and Monte Carlo, especially at high $p_t$, give confidence that the $p_t$ resolution is simulated correctly in the Monte Carlo. In particular, the agreement in the region above the kinematic edge of 2.3 GeV/c indicates that no unsimulated tails are present in the data. In section 6.2 this spectrum is used to set a limit on the number of extra high $p_t$ $K^{\pm}$'s that could be produced by extra $p_t$ smearing.

# 5 $K^{\pm}$ $p_t$ Spectra

Figure 4 shows the $p_t$ spectra for identified $K^{\pm}$'s in the 1-Vertex and for all decays (the sum of 1- and 2-vertex). As for the $\mu^{\pm}$ spectra, the Monte Carlo is normalized to the data by the number of tagged $b$-hemispheres. Table 2 gives the number of $K^{\pm}$'s with $p_t > 1.8$ Gev observed in both samples. Both raw and "normalized" numbers of events are shown. Normalized numbers have been corrected for $K^{\pm}$ mis-identification and identification efficiency and are expressed as number of events per tagged $B$. They have not, however, been

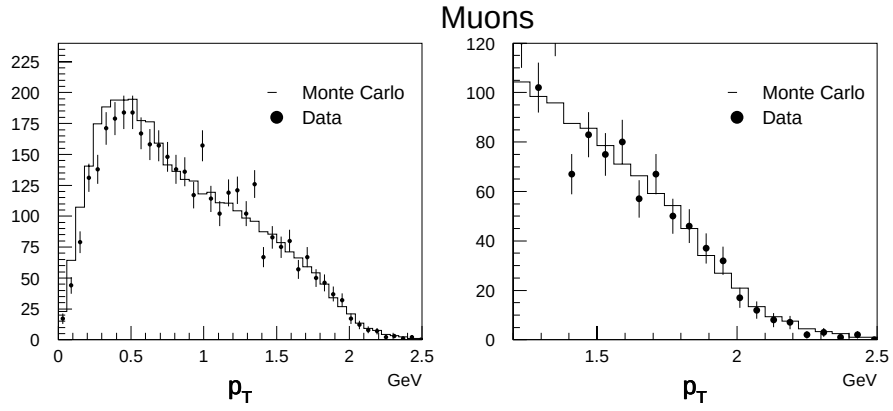


Figure 3: Comparison of data to Monte Carlo $p_t$ spectrum of identified muons.

corrected for $p_t$ resolution. Slightly more events are seen in the data than would be expected from $b \to c$ decays. These excesses, however, are small compared to what would be expected for BR($b \to sg$)= 10% and the $b \to sg$ model of Section 3. However, the statistical significance is insufficient to rule out a rather large BR($b \to sg$) somewhat less than 10%

# 6 Systematic Errors on Background Calculation

The calculation of the expected background of high $p_t$ $K^{\pm}$'s in the 1-vertex sample is subject to a number of possible systematic errors. Table 3 list the sources of background events as predicted by the Monte Carlo and gives an estimate of the systematic error of each source. These will be discussed in the following sections.

## 6.1 $B$ Decay Modeling

As can be seen from Table 3, the dominant source of true high $p_t$ $K^{\pm}$'s is from the decay of $D^0$'s produced in $B$ decays. Only $D^0$'s that are produced with

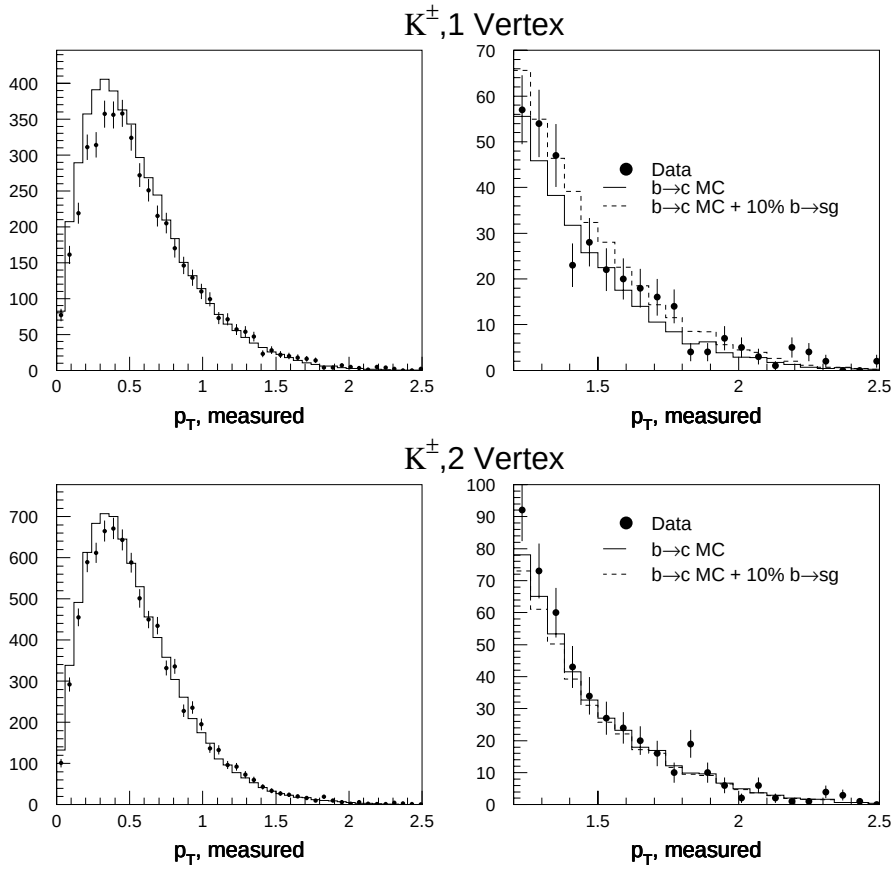


Figure 4: Comparison of data to Monte Carlo $p_t$ spectrum of identified $K^{\pm}$'s in the 1- and 2- vertex samples. The solid line shows the Monte Carlo predicted spectrum of standard $b \to c$ decays. The dashed line shows the predicted spectrum for BR($b \to sg$)=10% with $b \to sg$ generated as described in Section 3.

| $K^{\pm}$,$p_t > 1.8$ | 1 vertex | | All | |
|---|---|---|---|---|
| | Raw | Normalized | Raw | Normalized |
| Data | 37.0 | $1.82 \times 10^{-3}$ | 93.0 | $4.54 \times 10^{-3}$ |
| $b \to c$ MC | 29.0 | $1.32 \times 10^{-3}$ | 78.2 | $3.61 \times 10^{-3}$ |
| Difference | $8.0 \pm 6.1$ | $(5.0 \pm 3.8) \times 10^{-4}$ | $14.8 \pm 9.6$ | $(9.2 \pm 6.0) \times 10^{-4}$ |
| BR($b \to sg$)=10% | 24.0 | $1.5 \times 10^{-3}$ | 33.3 | $1.8 \times 10^{-3}$ |
| $b \to sg$ Gen. | | | | $1.1 \times 10^{-2}$ |
| $b \to c$ Gen. | | | | $2.4 \times 10^{-3}$ |

Table 2: Comparison of number of high $p_t$ $K^{\pm}$'s expected and observed in the 1-vertex sample and for all decays (the sum of 1- and 2-vertex samples). The number expected BR($b \to sg$)= 10% and the $b \to sg$ model of Section 3 is also shown. See the text for explanation of the Normalized columns. Monte Carlo generator level production of true high-$p_t$ $K^{\pm}$'s is shown for the $b \to sg$ generator and for the $b \to c$ generator.

high momentum in the $B$ rest frame and then decay with a high momentum $K^{\pm}$ in their own rest frame are likely to lead to a high $p_t$ $K^{\pm}$. It is therefore crucial to know the spectrum of $D^0$'s produced in $B$ decays and the spectrum of $K^{\pm}$'s produced in $D^0$. The former has been well measured by the CLEO collaboration [20] and the latter is simplified by the fact that the high-$p_t$ $K^{\pm}$'s are produced by a relatively small number of two-body decay modes, all of which are well measured. The SLD $B$-decay model is based on the CLEO model [17] and has been tuned to match this data.

The systematic errors from the knowledge of the $D^0$ spectrum can thus be calculated by scaling up each bin by its relative error and calculating the number of additional high $p_t$ $K^{\pm}$'s that would result. Figure 5 shows the CLEO spectrum that was used as well as the spectrum of $D^0$ momentum in the $B$ rest frame that produced the high $p_t$ $K^{\pm}$'s. Scaling up this spectrum by the CLEO errors gives approximately 12 % more high $p_t$ $K^{\pm}$'s. Similarly, scaling up the branching ratios of the four most important $D^0$ decay modes ($D^0 \to K^-\pi^+$,$D^0 \to K^-\rho^+$,$D^0 \to K^{*-}\pi^+$,$D^0 \to \bar{K}^{*0}\pi^0$) by their relative error, gives approximately 10 % more high $p_t$ $K^{\pm}$'s.

Another significant source of uncertainty in the modeling of $B$-decays is

| Source | | | | Error |
|---|---|---|---|---|
| Mis-ID | | 7.8 | | 1.5 |
| | Pion | | 2.3 | |
| | Lepton | | 4.3 | |
| | Proton | | 1.2 | |
| Fragmentation | | 0.0 | | |
| udsc | | 0.0 | | |
| From B | | 3.7 | | |
| | $B_s$ | | 0.3 | |
| | Cabibbo Suppressed | | 2.4 | 2.4 |
| | s quark popping | | 0.2 | |
| | Double Charm | | 0.0 | |
| | Charmonium | | 0.7 | |
| From D | | 17.5 | | |
| | $D^0$ | | 13.6 | $1.7 \oplus 1.4$ |
| | $D^+$ | | 1.2 | |
| | $D_s$ | | 2.7 | |
| From $V_{ub}$ | | | | $< 2.1$ |
| From $b \to s\gamma$ | | | | $< 1.1$ |
| MC statistics | | | | 1.5 |
| $K^{\pm}$ID eff. | | | | 2.7 |
| $p_t$ smear | | | | 2.7 |
| Total | | 29.0 | | 5.9 |

Table 3: Background sources for 1-vertex $K^{\pm}$'s with $p_t > 1.8$ and their estimated systematic errors.

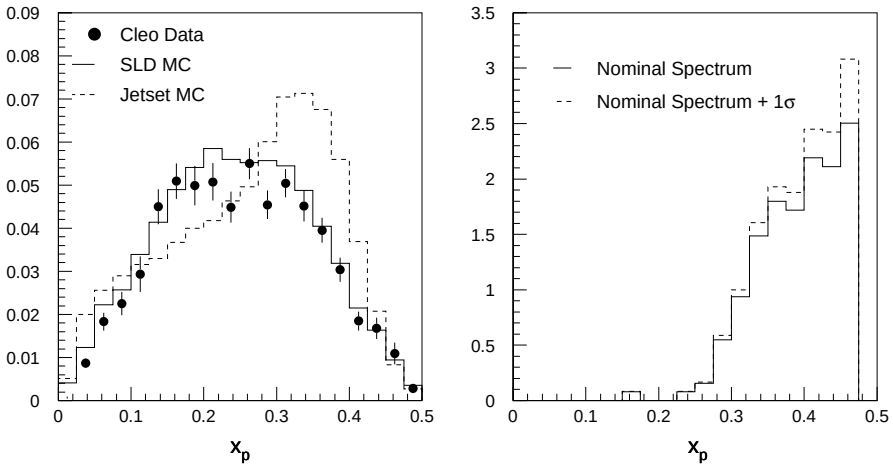


Figure 5: The first plot is the CLEO measured spectrum of $D^0$'s produced in $B$ decay plotted as a function of the scaled momentum, which is defined as $x = p/4.950\,Gev/c$. Also shown is this spectrum as generated by the SLD $B$-decay model and the JETSET default $B$-decay model. The second is the scaled momentum of $D^0$'s that produced high $p_t$ $K^{\pm}$'s. The solid line is for the nominal $D^0$ spectrum, and the dashed line is for the spectrum that is produced by scaling up each bin by its relative error.

the Cabibbo suppressed modes, *i.e.* those where $W^- \to \bar{u}s$ such as $B^+ \to \bar{D}^0 K^+$. These modes have mostly not been measured and are not properly included in the SLD Monte Carlo. Therefore, the analogous Cabibbo-allowed modes are used and the expected Cabibbo suppression factor of 0.05 is applied. A 100 % systematic error is taken to reflect the large uncertainty of the branching ratios of these modes. Contributions from other exotic effects such as $V_{ub}$ and $b \to s\gamma$ are small.

## 6.2 $p_t$ Measurement

The error on the measurement of $p_t$ is dominated by the measurement of the $B$-flight direction. The $p_t$ resolution is thus proportional to the total momentum of the track. In Monte Carlo, it is found the constant of proportionality is approximately 0.01. Therefore, the $p_t$ of a 10 Gev/c track is measured with an error of approximately 0.1 Gev/c. To determine a systematic error

associated with the $p_t$ measurement, the $p_t$ resolution in the Monte Carlo is artificially smeared until the Monte Carlo $\mu^{\pm}$ spectrum shown in Figure 3 no longer agrees with data. It is found that the $p_t$ resolution can be smeared by about 50 % above nominal before this occurs. Adding this additional smearing to the Monte Carlo $K^{\pm}$ spectrum gives 10 % additional high $p_t$ $K^{\pm}$'s.

### 6.3 Kaon Identification and Mis-Identification Efficiency

As shown in Table 3, 7.8 of the 29.0 high $p_t$ "$K^{\pm}$'s" in the Monte Carlo are actually mis-identified particles of other types. It is found that the mis-identification rate in data is higher than in Monte Carlo. The effect is calibrated by matching the mis-identification rate observed in data of a sample of $\pi^{\pm}$'s produced in $\mathrm{K}^0_{\mathrm{S}}$ decays. The systematic error of mis-identification is taken to be the whole adjustment made by this calibration procedure.

The identification efficiency of true $K^{\pm}$'s is checked in the data with $D^0 \to K^-\pi^+$ decays. The current statistics do not allow a calibration to be applied based on this data, but a conservative systematic error of 10% is taken.

## 7 Conclusion

We have performed an inclusive search for enhanced $b \to sg$ decays in 300,000 $Z^0$ decays taken during 1993-1997 by analysing the excess production of high $p_t$ $K^{\pm}$'s compared to standard $b \to c$ Monte Carlo. The preliminary observation of data excess of $p_t > 1.8$ GeV/c $K^{\pm}$'s in the 1-vertex sample yields a result of $8.0 \pm 6.1 \pm 5.9$ events over an expected background of 29 events. This corresponds to a $K^{\pm}$ identification efficiency corrected high $p_t$ production excess of $(5.0 \pm 3.8 \pm 3.6) \times 10^{-4}$ per $B$ decay. This corresponds to a statistical precision of $\pm 2.5\%$ on $b \to sg$ branching ratio for a particular set of choices of $b \to sg$ model parameters.

We have demonstrated that this measurement technique already has interesting statistical precision to test the hypothesis of largely enhanced $b \to sg$ branching ratio at 10% level, even with a rather small input data sample. Data taken in 1998 will be added in the near future which will approximately double the data statistics. A significant fraction of the background system-

atic uncertainties due to detector effects will also improve with increased data statistics. However, some significant effort on $b \to sg$ theoretical models is still needed to evaluate the uncertainties in the $b \to sg$ signal size for high $p_t$ kaon production before this result can be translated into an upper limit of $b \to sg$ branching ratio.

# 8 Acknowledgements

We thank the personnel of the SLAC accelerator department and the technical staffs of our collaborating institutions for their outstanding efforts. We also thank Alex Kagan for providing the $b \to sg$ model and for many useful discussions. This work was supported by the U.S. Department of Energy and National Science Foundation, the UK Particle Physics and Astronomy Research Council, the Istituto Nazionale di Fisica Nucleare of Italy, the Japan-US Cooperative Research Project on High Energy Physics, and the Korea Science and Engineering Foundation.

# References

[1] A. Lenz, U. Nierste, and G. Ostermaier, hep-ph/9802202;
A. Lenz, U. Nierste, and G. Ostermaier, *Phys. Rev.* D **56**, 7228 (1997).

[2] A.L.Kagan, *Phys. Rev.* D **51**, 6196 (1995);
M. Ciuchini, E. Gabrielli and G. F. Giudice, *Phys. Lett.* **B388**, 353 (1996);
B.G. Grzadkowski and W.-S. Hou, *Phys. Lett* B **272**, 383 (1991).

[3] CLEO Collaboration, *Contribution PA05-73 to the XXVIII International Conference on High Energy Physics, July 25-31, 1996, Warsaw, Poland.*
CLEO Collaboration, T. E. Browder *et al.*, hep-ex/9804018, Apr/1998.

[4] D. Atwood and A. Soni, *Phys. Lett* B **405**, 150 (1997);
W.-S. Hou and B. Tseng, *Phys. Rev. Let.* **80**, 434 (1998);
A.L. Kagan and A.A. Petrov, hep-ph 9707354.

[5] CLEO Collaboration, B. H. Behrens *et al.*, *Phys. Rev. Let.* **80**, 3710 (1998).

[6] A. Ali and C. Greub, *Phys. Rev.* D **57**, 2996 (1998);
N. G. Deshpande, B. Dutta, S. Oh, *Phys. Rev.* D **57**, 5723 (1998);
H. Y. Cheng and B. Tseng, hep-ph/9803457.

[7] SLD Collab., K. Abe. *et al.*, *Phys. Rev. Let.* **78**, 3442 (1997),Erratum-ibid.79:959,1997.

[8] T. Sjöstrand, *Comp. Phys. Comm.* **82**, 74 (1994)

[9] A. Kagan and J. Rathsmann, hep-ph/9701300

[10] M. D. Hildreth *et al.*, *Nucl. Instr. & Meth.* **A367**, 111 (1995); & IEEE Trans. Nucl. Sci. **42**, 451 (1995).

[11] G. Agnew *et al.*, SLAC-PUB-5906, *Proceedings of the 26th International Conference on High Energy Physics, Dallas, Texas, USA*

[12] K. Abe *et al.*, *Nucl. Instr. & Meth.* **A400**, 287 (1997).

[13] D. Axen *et al.*, *Nucl. Instr. & Meth.* **A238**, 472 (1993).

[14] SLD Collab.: K. Abe *et al.*, *Phys. Rev.* D **53**, 1023 (1996).

[15] K. Abe *et al.*, *Nucl. Instr. & Meth.* **A343**, 74 (1994).

[16] Particle Data Group, *Phys. Rev.* D **50**, 1173 (1994).

[17] CLEO $B$ decay model provided by P. Kim and the CLEO Collaboration.

[18] N. Isgur, D. Scora, B. Grinstein, and M. B. Wise, *Phys. Rev.* D **39**, 799 (1989).

[19] CLEO Collab.: B. Barish *et al.*, *Phys. Rev. Let.* **76**, 1570 (1996).

[20] CLEO Collab.: L. Gibbons *et al.*, *Phys. Rev.* D **56**, 3783 (1997).

[21] CLEO Collab.: G. Crawford *et al.*, *Phys. Rev.* D **45**, 752 (1992).

[22] CLEO Collab.: D. Bortoletto *et al.*, *Phys. Rev.* D **45**, 21 (1992).

[23] ARGUS Collab.: H. Albrecht *et al.*, *Z. Phys.* C **58**, 191 (1993). ARGUS Collab.: H. Albrecht *et al.*, *Z. Phys.* C **62**, 371 (1994).

[24] SLD Collab., K. Abe. *et al.*, *Phys. Rev. Let.* **80**, 660 (1998);
SLD Collab., K. Abe. *et al.*, SLAC-PUB-7585, *Contribution EPS-118 to the International Europhysics Conference on High Energy Physics (HEP-97), Aug 19-26, 1997, Jerusalem, Israel.*

[25] D. Jackson, *Nucl. Instr. & Meth.* **A388**, 247 (1997).

[26] K. Abe. *et al.*, *Nucl. Instr. & Meth.* **A371**, 195 (1996); K. Abe. *et al.*, SLAC-PUB-7766, *submitted to Phys. Rev. D*, May/1998.

[27] SLD Collab., K. Abe. *et al.*, SLAC-PUB-7630, *Contribution EPS-123 to the International Europhysics Conference on High Energy Physics (HEP-97), Aug 19-26, 1997, Jerusalem, Israel.*

## **List of Authors


K. Abe,[2] K. Abe,[19] T. Abe,[27] I.Adam,[27] T. Akagi,[27] N. J. Allen,[4]
A. Arodzero,[20] W.W. Ash,[27] D. Aston,[27] K.G. Baird,[15] C. Baltay,[37]
H.R. Band,[36] M.B. Barakat,[14] O. Bardon,[17] T.L. Barklow,[27]
J.M. Bauer,[16] G. Bellodi,[21] R. Ben-David,[37] A.C. Benvenuti,[3]
G.M. Bilei,[23] D. Bisello,[22] G. Blaylock,[15] J.R. Bogart,[27] B. Bolen,[16]
G.R. Bower,[27] J. E. Brau,[20] M. Breidenbach,[27] W.M. Bugg,[30]
D. Burke,[27] T.H. Burnett,[35] P.N. Burrows,[21] A. Calcaterra,[11]
D.O. Caldwell,[32] D. Calloway,[27] B. Camanzi,[10] M. Carpinelli,[24]
R. Cassell,[27] R. Castaldi,[24] A. Castro,[22] M. Cavalli-Sforza,[33]
A. Chou,[27] E. Church,[35] H.O. Cohn,[30] J.A. Coller,[5] M.R. Convery,[27]
V. Cook,[35] R. Cotton,[4] R.F. Cowan,[17] D.G. Coyne,[33] G. Crawford,[27]
C.J.S. Damerell,[25] M. N. Danielson,[7] M. Daoudi,[27] N. de Groot,[27]
R. Dell'Orso,[23] P.J. Dervan,[4] R. de Sangro,[11] M. Dima,[9]
A. D'Oliveira,[6] D.N. Dong,[17] P.Y.C. Du,[30] R. Dubois,[27]
B.I. Eisenstein,[12] V. Eschenburg,[16] E. Etzion,[36] S. Fahey,[7]
D. Falciai,[11] C. Fan,[7] J.P. Fernandez,[33] M.J. Fero,[17] K.Flood,[15]
R. Frey,[20] T. Gillman,[25] G. Gladding,[12] S. Gonzalez,[17] E.L. Hart,[30]
J.L. Harton,[9] A. Hasan,[4] K. Hasuko,[31] S. J. Hedges,[5]
S.S. Hertzbach,[15] M.D. Hildreth,[27] J. Huber,[20] M.E. Huffer,[27]
E.W. Hughes,[27] X.Huynh,[27] H. Hwang,[20] M. Iwasaki,[20]
D. J. Jackson,[25] P. Jacques,[26] J.A. Jaros,[27] Z.Y. Jiang,[27]
A.S. Johnson,[27] J.R. Johnson,[36] R.A. Johnson,[6] T. Junk,[27]
R. Kajikawa,[19] M. Kalelkar,[26] Y. Kamyshkov,[30] H.J. Kang,[26]
I. Karliner,[12] H. Kawahara,[27] Y. D. Kim,[28] R. King,[27] M.E. King,[27]
R.R. Kofler,[15] N.M. Krishna,[7] R.S. Kroeger,[16] M. Langston,[20]
A. Lath,[17] D.W.G. Leith,[27] V. Lia,[17] C.-J. S. Lin,[27] X. Liu,[33]
M.X. Liu,[37] M. Loreti,[22] A. Lu,[32] H.L. Lynch,[27] J. Ma,[35]
G. Mancinelli,[26] S. Manly,[37] G. Mantovani,[23] T.W. Markiewicz,[27]
T. Maruyama,[27] H. Masuda,[27] E. Mazzucato,[10] A.K. McKemey,[4]
B.T. Meadows,[6] G. Menegatti,[10] R. Messner,[27] P.M. Mockett,[35]
K.C. Moffeit,[27] T.B. Moore,[37] M.Morii,[27] D. Muller,[27] V.Murzin,[18]
T. Nagamine,[31] S. Narita,[31] U. Nauenberg,[7] H. Neal,[27]
M. Nussbaum,[6] N.Oishi,[19] D. Onoprienko,[30] L.S. Osborne,[17]
R.S. Panvini,[34] H. Park,[20] C. H. Park,[29] T.J. Pavel,[27] I. Peruzzi,[11]
M. Piccolo,[11] L. Piemontese,[10] E. Pieroni,[24] K.T. Pitts,[20]
R.J. Plano,[26] R. Prepost,[36] C.Y. Prescott,[27] G.D. Punkar,[27]
J. Quigley,[17] B.N. Ratcliff,[27] T.W. Reeves,[34] J. Reidy,[16]

P.L. Reinertsen,[33] P.E. Rensing,[27] L.S. Rochester,[27] P.C. Rowson,[8] J.J. Russell,[27] O.H. Saxton,[27] T. Schalk,[33] R.H. Schindler,[27] B.A. Schumm,[33] J. Schwiening,[27] S. Sen,[37] V.V. Serbo,[36] M.H. Shaevitz,[8] J.T. Shank,[5] G. Shapiro,[13] D.J. Sherden,[27] K. D. Shmakov,[30] C. Simopoulos,[27] N.B. Sinev,[20] S.R. Smith,[27] M. B. Smy,[9] J.A. Snyder,[37] H. Staengle,[9] A. Stahl,[27] P. Stamer,[26] R. Steiner,[1] H. Steiner,[13] M.G. Strauss,[15] D. Su,[27] F. Suekane,[31] A. Sugiyama,[19] S. Suzuki,[19] M. Swartz,[27] A. Szumilo,[35] T. Takahashi,[27] F.E. Taylor,[17] J. Thom,[27] E. Torrence,[17] N. K. Toumbas,[27] A.I. Trandafir,[15] J.D. Turk,[37] T. Usher,[27] C. Vannini,[24] J. Va'vra,[27] E. Vella,[27] J.P. Venuti,[34] R. Verdier,[17] P.G. Verdini,[24] S.R. Wagner,[27] D. L. Wagner,[7] A.P. Waite,[27] Walston, S.,[20] J.Wang,[27] C. Ward,[4] S.J. Watts,[4] A.W. Weidemann,[30] E. R. Weiss,[35] J.S. Whitaker,[5] S.L. White,[30] F.J. Wickens,[25] B. Williams,[7] D.C. Williams,[17] S.H. Williams,[27] S. Willocq,[27] R.J. Wilson,[9] W.J. Wisniewski,[27] J. L. Wittlin,[15] M. Woods,[27] G.B. Word,[34] T.R. Wright,[36] J. Wyss,[22] R.K. Yamamoto,[17] J.M. Yamartino,[17] X. Yang,[20] J. Yashima,[31] S.J. Yellin,[32] C.C. Young,[27] H. Yuta,[2] G. Zapalac,[36] R.W. Zdarko,[27] J. Zhou.[20]

*(The SLD Collaboration)*

[1] *Adelphi University, South Avenue- Garden City,NY 11530,*
[2] *Aomori University, 2-3-1 Kohata, Aomori City, 030 Japan,*
[3] *INFN Sezione di Bologna, Via Irnerio 46 I-40126 Bologna, Italy,*
[4] *Brunel University, Uxbridge, Middlesex - UB8 3PH United Kingdom,*
[5] *Boston University, 590 Commonwealth Ave. - Boston,MA 02215,*
[6] *University of Cincinnati, Cincinnati,OH 45221,*
[7] *University of Colorado, Campus Box 390 - Boulder,CO 80309,*
[8] *Columbia University, Nevis Laboratories P.O.Box 137 - Irvington,NY 10533,*
[9] *Colorado State University, Ft. Collins,CO 80523,*
[10] *INFN Sezione di Ferrara, Via Paradiso,12 - I-44100 Ferrara, Italy,*
[11] *Lab. Nazionali di Frascati, Casella Postale 13 I-00044 Frascati, Italy,*
[12] *University of Illinois, 1110 West Green St. Urbana,IL 61801,*
[13] *Lawrence Berkeley Laboratory, Dept.of Physics 50B-5211 University of California- Berkeley, CA 94720,*
[14] *Louisiana Technical University, Dept. of Physics, Ruston, LA 71272,*
[15] *University of Massachusetts, Amherst,MA 01003,*

[16] *University of Mississippi, University,MS 38677,*
[17] *Massachusetts Institute of Technology, 77 Massachusetts Avenue Cambridge, MA 02139,*
[18] *Moscow State University, Institute of Nuclear Physics 119899 Moscow, Russia,*
[19] *Nagoya University, Nagoya 464 Japan,*
[20] *University of Oregon, Department of Physics Eugene,OR 97403,*
[21] *Oxford University, Oxford, OX1 3RH, United Kingdom,*
[22] *Universita di Padova, Via F. Marzolo,8 I-35100 Padova, Italy,*
[23] *Universita di Perugia, Sezione INFN, Via A. Pascoli I-06100 Perugia, Italy,*
[24] *INFN, Sezione di Pisa, Via Livornese,582/AS Piero a Grado I-56010 Pisa, Italy,*
[25] *Rutherford Appleton Laboratory, Chiton,Didcot - Oxon OX11 0QX United Kingdom,*
[26] *Rutgers University, Serin Physics Labs Piscataway,NJ 08855-0849,*
[27] *Stanford Linear Accelerator Center, 2575 Sand Hill Road Menlo Park,CA 94025,*
[28] *Sogang University, Ricci Hall Seoul, Korea,*
[29] *Soongsil University, Dongjakgu Sangdo 5 dong 1-1 Seoul, Korea 156-743,*
[30] *University of Tennessee, 401 A.H. Nielsen Physics Blg. - Knoxville, Tennessee 37996-1200,*
[31] *Tohoku University, Bubble Chamber Lab. - Aramaki - Sendai 980, Japan,*
[32] *U.C. Santa Barbara, 3019 Broida Hall Santa Barbara,CA 93106,*
[33] *U.C. Santa Cruz, Santa Cruz,CA 95064,*
[34] *Vanderbilt University, Stevenson Center,Room 5333 P.O.Box 1807,Station B Nashville,TN 37235,*
[35] *University of Washington, Seattle,WA 98105,*
[36] *University of Wisconsin, 1150 University Avenue Madison,WS 53706,*
[37] *Yale University, 5th Floor Gibbs Lab. - P.O.Box 208121 - New Haven,CT 06520-8121.*